Publications of the Korean Astronomical Society
30: 159 ∼ 161, 2015 September

pISSN: 1225-1534
eISSN: 2287-6936
http://dx.doi.org/10.5303/PKAS.2015.30.2.159

PHYSICAL AND CHEMICAL PROPERTIES OF PLANETARY NEBULAE WITH WR-TYPE NUCLEI

Ashkbiz Danehkar[1], Roger Wesson[2], Amanda I. Karakas[3], and Quentin A. Parker[1,4]
[1]Department of Physics and Astronomy, Macquarie University, Sydney, NSW 2109, Australia
[2]European Southern Observatory, Alonso de Córdova 3107, Casilla 19001, Santiago, Chile
[3]Research School of Astronomy & Astrophysics, Australian National University, Canberra ACT 2611, Australia
[4]Australian Astronomical Observatory, PO Box 915, North Ryde, NSW 1670, Australia

E-mail: ashkbiz.danehkar@students.mq.edu.au
(Received November 30, 2014; Reviced May 31, 2015; Aaccepted June 30, 2015)

ABSTRACT

We have carried out optical spectroscopic measurements of emission lines for a sample of Galactic planetary nebulae with Wolf-Rayet (WR) stars and weak emission-line stars (*wels*). The plasma diagnostics and elemental abundance analysis have been done using both collisionally excited lines (CELs) and optical recombination lines (ORLs). It was found that the abundance discrepancy factors (ADF ≡ ORL/CEL) are closely correlated with the difference between temperatures derived from forbidden lines and those from He I recombination lines, implying the existence of H-deficient materials embedded in the nebula. The Hβ surface brightness correlations suggest that they might be also related to the nebular evolution.

Key words: ISM: abundances – planetary nebulae: general – stars: Wolf-Rayet

1. INTRODUCTION

Observations of planetary nebulae (PNe) are used to determine the composition of the interstellar medium (e.g. Kingsburgh & Barlow, 1994), and to probe the physics of AGB stars (e.g. Karakas et al., 2009). Collisionally excited lines (CELs) have been extensively used to derive the abundances of heavy elements (see e.g. Kingsburgh & Barlow, 1994; Liu et al., 2004). Alternatively, optical recombination lines (ORLs) have a much weaker dependence on temperature, thus resulting in more reliable abundance analyses. However, the abundances derived using the ORL method are systematically higher than those derived from CELs in PNe (e.g. Tsamis et al., 2004; Wesson & Liu, 2004; Wesson et al., 2005). Previously, Peimbert (1967) found a difference between [O III] CEL and H I Balmer jump (BJ) temperatures with $T_e([O\,III]) > T_e(BJ)$. Moreover, Wesson et al. (2005) found that $T_e([O\,III]) > T_e(BJ) > T_e(He\,I) > T_e(O\,II)$, which was predicted by the two-phase models (Liu et al., 2004), containing some cold ($T_e \sim 10^3$ K) H-deficient materials, embedded in the warm ($T_e \sim 10^4$ K) gas of normal abundance.

For this study, we carried out optical integral field observations of a sample of PNe (see Danehkar, 2014) using the Wide Field Spectrograph (WiFeS; Dopita et al., 2010) on the ANU 2.3 telescope. Our observations were carried out with the B7000/R7000 grating combination ($R \sim 7000$). We acquired a series of bias, dome and flat-field frames, twilight sky flats, arc lamp exposures, wire frames, spectrophotometric standard stars for flat-fielding, wavelength calibration, spatial calibration and flux calibration as (described in detail by Danehkar et al., 2013, 2014). Suitable sky windows were selected from the science data for sky subtraction.

2. PLASMA DIAGNOSTICS

Nebular electron temperatures T_e and densities N_e were obtained from the intrinsic intensities of CELs by solving level populations for an n-level ($\geqslant 5$) atomic model using the EQUIB code.

Figure 1 (top-left panel) shows the logarithmic electron density $\log N_e([S\,II])$ plotted against the logarithmic intrinsic nebular Hβ surface brightness. The dotted line represents a linear fit to the 18 PNe in our sample, which have a strong linear correlation: $\log N_e([S\,II]) = (4.59 \pm 0.23) + (0.5 \pm 0.1) \log S(H\beta)$, where $S(H\beta)$ is the dereddened nebular Hβ surface brightness. It is seen that $S(H\beta) \propto N_e^2$, in agreement with the theoretical relation of O'Dell (1962).

Figure 1 (top-right panel) plots T_e versus the excitation class (EC; Dopita & Meatheringham, 1990). A trend of increasing T_e with increasing EC is seen. A linear fit to $T_e([O\,III])$ and as a function of EC yields $T_e([O\,III]) = (5997 \pm 592) + (626.84 \pm 100.57)\,EC$. The electron temperatures of high-excitation PNe are typically higher than low-excitation PNe, which can be explained by the radiation from the central stars.

3. ABUNDANCE ANALYSIS

We determined ionic abundances for CELs by solving the statistical equilibrium equations for each ion using

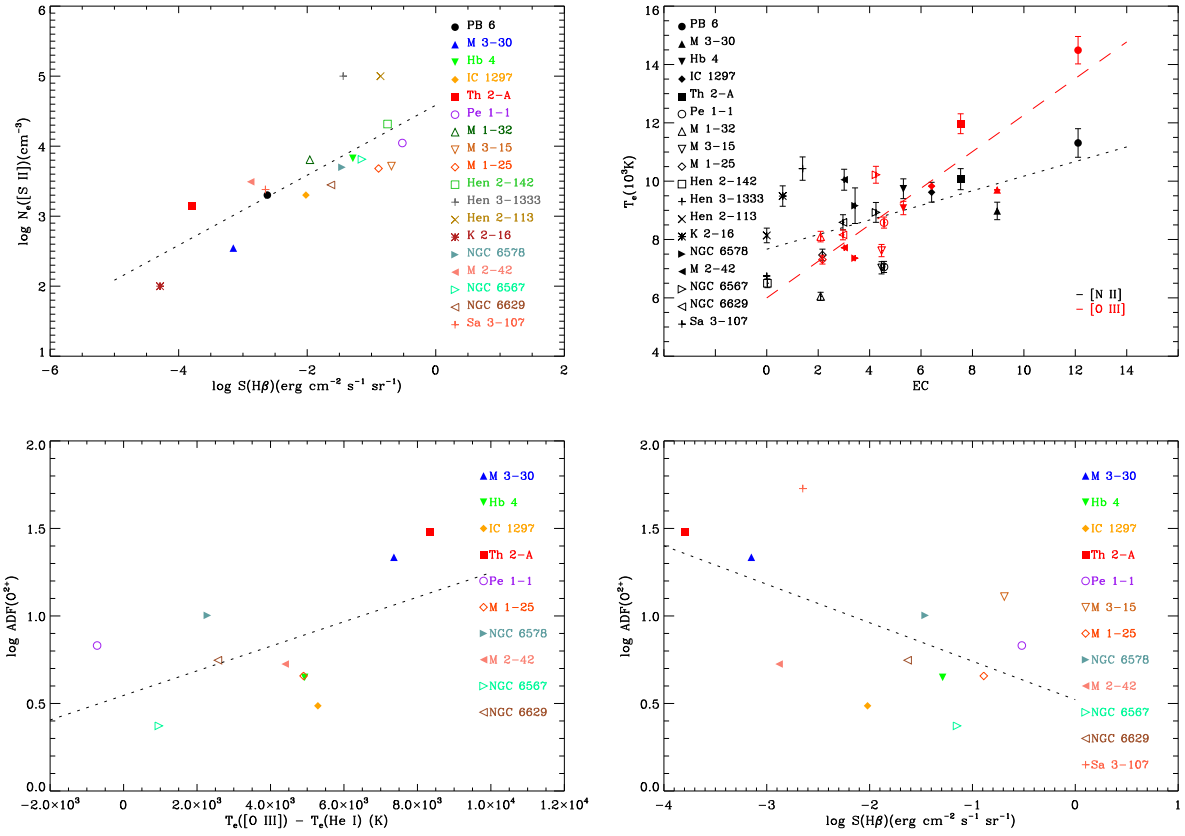

Figure 1. Top-Left panel: The logarithmic electron density plotted against the logarithmic nebular surface brightness. Top-Right panel: Variation of the electron temperature along the excitation class (EC); the dotted and dashed lines for T_e([N II]) and T_e([O III]). Bottom-Left panel: The difference between the electron temperatures and the helium temperatures plotted against the ADF for O^{2+}. Bottom-Right panel: The ADF for O^{2+} plotted against the logarithmic nebular surface brightness.

the EQUIB code, giving level population and line emissivities for specified T_e and N_e. We determined ionic abundances of ORLs for our sample where adequate observed lines were available.

Figure 1 (bottom-left panel) shows the logarithmic abundance discrepancy factor (ADF) for O^{2+}, defined as $\log \mathrm{ADF}(O^{2+}) \equiv \log(O^{2+}/H^+)_{\mathrm{ORL}} - \log(O^{2+}/H^+)_{\mathrm{CEL}}$ plotted against the difference between the [O III] forbidden-line and the He I recombination-line temperatures $\Delta T_{[\mathrm{O\,III}]} \equiv T_e([\mathrm{O\,III}]) - T_e(\mathrm{He\,I})$. A linear fit to the 10 PNe plotted in the figure yields $\log \mathrm{ADF}(O^{2+}) = (0.55 \pm 0.18) + (7.0 \pm 3.7) \times 10^{-5} \times \Delta T_{[\mathrm{O\,III}]}(\mathrm{K})$.

In Figure 1 (bottom-right panel) we plot the O^{2+}/H^+ ADF as a function of the intrinsic nebular Hβ surface brightness $\log S(\mathrm{H}\beta)$. A linear fit to the 12 PNe plotted in the figure yields $\log \mathrm{ADF}(O^{2+}) = (0.52 \pm 0.22) - (0.22 \pm 0.10) \log S(\mathrm{H}\beta)$.

4. CONCLUSIONS

In conclusion, there is a dependence of the nebular ORL/CEL ADFs on the difference between temperatures derived from forbidden lines and those from He I recombination lines, T_e(CELs) − T_e(He I), and the intrinsic nebular surface brightness, $\log S(\mathrm{H}\beta)$. It has been known that the ADFs are closely correlated with the difference between T_e([O III]) and T_e(BJ) (Liu et al., 2004; Tsamis et al., 2004; Wesson et al., 2005). These correlations suggest that the observed ORLs may originate from cold ionized gas located in metal-rich clumps inside the diffuse warm nebula, but the origin of such inclusions is as yet unknown. The correlation between the nebular ADFs and the intrinsic Hβ surface brightness found here is consistent with previous results (Liu et al., 2004; Tsamis et al., 2004). This suggests that the abundance discrepancy might be related to the nebular evolution, as it is higher in old evolved PNe.

ACKNOWLEDGMENTS

AD acknowledges a student travel assistance from the Astronomical Society of Australia (ASA) and a travel grant from the International Astronomical Union (IAU).

REFERENCES

Danehkar, A., 2014, PhD thesis, Macquarie University
Danehkar, A., Parker, Q. A., & Ercolano, B., 2013, Observations and Three-dimensional Ionization Structure of the Planetary Nebula SuWt 2, MNRAS, 434, 1513
Danehkar, A., Todt, H., Ercolano, B. & Kniazev, A. Y., 2014, Observations and Three-dimensional Photoioniza-

tion Modelling of the Wolf-Rayet Planetary Nebula Abell 48, MNRAS, 439, 3605
Dopita, M. A. & Meatheringham, S. J. 1990, The Evolutionary Sequence of Planetary Nebulae, ApJ, 357, 140
Dopita, M. et al., 2010, The Wide Field Spectrograph (WiFeS): performance and data reduction, ap&ss, 327, 245
Karakas, A. I., van Raai, M. A., Lugaro, M., Sterling N. C., & Dinerstein. H. L. 2009, ApJ, 690, 1130
Kingsburgh, R. L. & Barlow, M. J., 1994, Nucleosynthesis Predictions for Intermediate-Mass Asymptotic Giant Branch Stars: Comparison to Observations of Type I Planetary Nebulae, MNRAS, 271, 257
Liu, Y., Liu, X. -W., Barlow, M. J., & Luo, S. -G., 2004, Chemical Abundances of Planetary Nebulae from Optical Recombination Lines - II. Abundances Derived from Collisionally Excited Lines and Optical Recombination Lines, MNRAS, 353, 1251
O'Dell, C. R., 1962, A Distance Scale for Planetary Nebulae Based on Emission-Line Fluxes, ApJ, 135, 371
Peimbert, M., 1967, Temperature Determinations of H II Regions, ApJ, 150, 825
Tsamis, Y. G., Barlow, M. J., Liu, X. -W., Storey, P. J., & Danziger, I. J., 2004, A deep survey of heavy element lines in planetary nebulae - II. Recombination-line abundances and evidence for cold plasma, MNRAS, 353, 953
Wesson, R. & Liu, X. -W., 2004, Physical conditions in the planetary nebula NGC 6543, MNRAS, 351, 1026
Wesson, R., Liu, X. -W., & Barlow, M. J., 2005, The abundance discrepancy - recombination line versus forbidden line abundances for a northern sample of galactic planetary nebulae, MNRAS, 362, 424